

Donor Acceptor Complexes of Noble Gases

Leonie Anna Mück,[†] Alexey Y. Timoshkin,^{*,‡} Moritz von Hopffgarten,[†] and Gernot Frenking[†]

Inorganic Chemistry Group, Department of Chemistry, St. Petersburg State University, University Pr. 26, Old Peterhof, 198504, Russia, and Philipps-Universität Marburg, Hans-Meerwein-Strasse, D-35032 Marburg, Germany

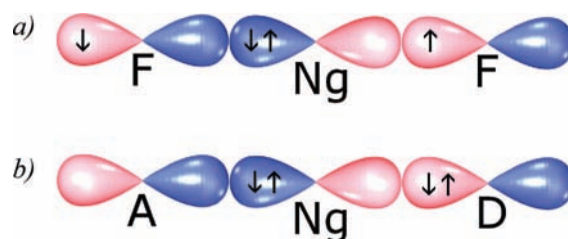
Received July 30, 2008; E-mail: alextim@AT11692.spb.edu; frenking@staff.uni-marburg.de

Abstract: Donor–acceptor (DA) complexes of noble gases (Ng) of the general type $A \leftarrow Ng \leftarrow D$ ($A =$ Lewis acid, $D =$ Lewis base) have been theoretically studied using *ab initio* and DFT methods. Chemical bonding in these compounds is realized via a 3-center 4-electron bond, which is formed by a lone pair of the noble gas, a lone pair of the donor molecule and a vacant orbital of the acceptor molecule. Detailed bonding analysis of the model compounds $F_3Al-Ng-NH_3$ reveals that Ng–ammonia interaction is repulsive due to Pauli repulsion. Bonding interaction between Ng and N is mostly electrostatic. In contrast, strong orbital interactions are responsible for the attractive interactions between Ng and AlF_3 . Due to the repulsive interactions with the donor molecule and a sizable reorganization energy of the acceptor molecule, optimization attempts of the $A \leftarrow Ng \leftarrow D$ compounds, which feature individual donor and acceptor molecules, always lead to the dissociation of the complex and eventual formation of free Ng. To overcome this obstacle, the concept of a rigid C_{3v} symmetric cryptand-type ligand, which features spatially separated pyramidalized donor and acceptor fragments, is introduced. Such “push–pull” ligands are predicted to *exothermically* form complexes with noble gases. These are the first examples of the thermodynamically stable Ar and Kr compounds. Application of the push–pull cryptand ligands featuring multiple (two and three) donor–acceptor induced chemical bonds is expected to yield stable complexes with virtually any electron-rich element in the periodic table.

Introduction

Noble gases are unique elements in the chemistry world. Due to the completeness of the outer electronic shell, in nature noble gases exist as individual atoms, which are generally inert and are not likely to be involved in chemical bonding. To force the formation of chemical bonds with noble gases, the help of strong oxidation agents, such as F_2 , or extreme activation (laser irradiation, electric discharge) with subsequent trapping of the reaction products in low temperature matrices is required. Since the first synthesis of xenon compounds by Bartlett^{1a} and Hoppe^{1b} in 1962, a variety of compounds featuring Ng–halogen, –oxygen, –sulfur, –nitrogen, and –carbon bonds have been isolated and characterized.² The chemistry of krypton has been reviewed by Lehmann, Mercier, and Schrobilgen in 2002.³ The formation of noble gas molecules in low temperature matrixes

Scheme 1. Possible Pathways of the 3-Center 4-Electron Bond Formation: (a) Case of the Noble Gas Difluorides $F-Ng-F$ and (b) Case of the Donor–Acceptor Complexes $A \leftarrow Ng \leftarrow D$



was reviewed by Gerber in 2004.⁴ An excellent critical review by Grochala on the recent progress of the noble gas chemistry has appeared recently.⁵

Noble gas compounds are usually metastable and highly reactive, readily evolving noble gases in their atomic form. The bonding situation in relatively stable species, such as NgF_2 , can be explained with the help of 3-center 4-electron bonds.⁶ The terminal fluorine atoms equally participate in bond formation, providing one singly occupied orbital each, while the Ng atom provides one of its lone pairs (Scheme 1a). However, there is another theoretical possibility for the realization of such a 3-center 4-electron bond via donor–acceptor interactions (Scheme

[†] Philipps-Universität Marburg.

[‡] St. Petersburg State University.

- (1) (a) Bartlett, N. *Proc. Chem. Soc.* **1962**, 218. (b) Hoppe, R.; Dähne, W.; Mattauch, H.; Rödder, K. M. *Angew. Chem.* **1962**, *74*, 903; *Angew. Chem., Int. Ed.* **1962**, *1*, 599.
- (2) (a) Greenwood, N. N.; Earnshaw, A. *Chemistry of the Elements*; Butterworth-Heinemann: Oxford, 2001; p 888. (b) Frohn, H.-J.; Bardin, V. V. *Organometallics* **2001**, *20*, 4750. (c) Pettersson, M.; Lundell, J.; Khriachtchev, L.; Isoniemi, E.; Räsänen, M. *J. Am. Chem. Soc.* **1998**, *120*, 7979. (d) Khriachtchev, L.; Tanskanen, H.; Lundell, J.; Pettersson, M.; Kiljunen, H.; Räsänen, M. *J. Am. Chem. Soc.* **2003**, *125*, 4696. (e) Khriachtchev, L.; Isokoski, K.; Cohen, A.; Räsänen, M.; Gerber, R. B. *J. Am. Chem. Soc.* **2008**, *130*, 6114.
- (3) Lehmann, J. F.; Mercier, H. P. A.; Schrobilgen, G. J. *Coord. Chem. Rev.* **2002**, *233–234*, 1.

(4) Gerber, R. B. *Annu. Rev. Phys. Chem.* **2004**, *55*.

(5) Grochala, W. *Chem. Soc. Rev.* **2007**, *36*, 1632.

(6) Collins, G. A. D.; Cruickshank, D. W. J.; Breeze, A. *J. Chem. Soc., Faraday Trans.* **1974**, *70*, 393.

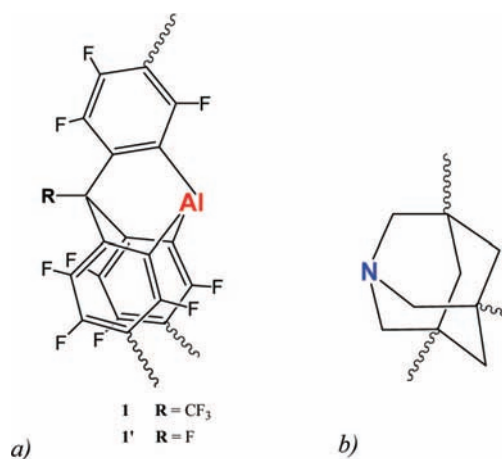
1b). In such a case both the noble gas atom and the donor molecule D contribute one lone pair each, while the acceptor A provides a vacant orbital. As an extreme example of the realization of such a bonding situation we can indicate HArF^7 and HKrF^8 molecules which have been produced by the HF photolysis in argon and krypton matrices. HNgF can be viewed as a donor–acceptor complex between H^+ , Ng, and F^- , where the proton acts as a hard Lewis acid, and F^- as a hard Lewis base. Theoretical analysis of these species revealed significant charge transfer from F^- to the HNg^+ moiety, electrostatic nature of the attraction between F and Ng, and covalent hydrogen–Ng interaction.⁹ Both HArF and HKrF are only metastable, due to exothermic dissociation into free Ng and HF (-559 and -473 kJ mol^{-1} for Ar and Kr, respectively, as computed at CCSD(T)/aug-cc-PVQZ//CCSD(T)/aug-cc-PVTZ level of theory).¹⁰ Recently, analogous Au(I) compounds of the type $\text{Au}^+-\text{Ng}-\text{F}^-$ (Ng = Ar, Kr, Xe) have been theoretically considered,¹¹ and a covalent bonding between Au and Ng has been established. It has also been shown that the interaction between a Au^+ cation and noble gases has a covalent component for Ar, Kr, and Xe.¹²

If the bonding situation shown in Scheme 1b is to be practically realized, one should suppress the possibility of the direct interactions between the donor and acceptor centers. In other words, to form a stable (“handy” or “bottleable”) compound, the reaction $\text{A}-\text{Ng}-\text{D} = \text{Ng} + \text{AD}$ should be completely avoided. We propose that this can be achieved by using novel push–pull cryptand ligands. Introduction of the rigid cage structure has been used to dramatically change the properties of compounds or stabilize unusual structures. For example, Bucher¹³ designed rigid C_3 symmetric organic bases featuring boron and nitrogen atoms as a molecular axis. He showed that the use of the C_3 symmetric $(\text{CH}_2)_3\text{N}$ bridge significantly reduces the conformational flexibility of the tris-8-quinolylborane and forces three nitrogen atoms in close proximity. Such compounds are predicted to be very strong proton acceptors.¹³

Ideally, a successfully designed ligand should be such that the Ng atom can be spontaneously introduced into the cage. It should have linear arrangement of the interacting donor and acceptor fragments (the $\text{A}-\text{Ng}-\text{D}$ angle should ideally be 180° , like in NgF_2). It should feature pyramidal donor and acceptor centers with a rigid connection between them that precludes direct DA interaction and provides small reorganization energy of the ligand upon complex formation. To facilitate complex formation with Ng, the acceptor center should have a large electron withdrawing ability.

In the present Article, tris(perfluoroaryl)aluminum and azaadamantane were used to construct a rigid cage with pyramidal acceptor and donor pockets (Scheme 2). Recently, we have demonstrated that fluorination dramatically increases Lewis acidity of group 13 aryls.¹⁴ Fluorinated pyramidal acceptors

Scheme 2. Pyramidalized Acceptor and Donor Binding Pockets Based on (a) Tris(perfluoroaryl)aluminum and (b) Azaadamantane with Wavy Lines Representing Positions of Bridging Carbene ($-\text{C}\equiv\text{C}-$)₃ Units



(Scheme 2a) are predicted to form very stable complexes with ammonia and azaadamantane (interaction energies ranging from -190 to -210 kJ mol^{-1}). Detailed evaluation of the fluorination degree on the acceptor properties of such pyramidalized acceptors will be presented elsewhere.¹⁵ A simple carbene ($-\text{C}\equiv\text{C}-$)₃ chain has been utilized to connect donor and acceptor pockets, resulting in C_{3v} symmetric push–pull cryptand ligand **1**. In preliminary computations, an analogue of **1** was considered, where CF_3 group on the acceptor pocket is substituted by a single F atom. This ligand will be denoted **1'**. We note that designed compounds **1** and **1'** are considered only as examples of rigid cryptand systems and not as prospective synthetic targets. The bonding situation in such compounds has been studied with the example of the $\text{F}_3\text{Al} \leftarrow \text{Ng} \leftarrow \text{NH}_3$ model systems with restricted tetrahedral geometry on both donor and acceptor molecules.

In the present Article, we for the first time report on the possibility of the existence of the *thermodynamically stable* donor–acceptor complexes of the type $\text{A} \leftarrow \text{Ng} \leftarrow \text{D}$ with cryptand ligands featuring neutral donor and acceptor centers. Due to the fact that the chemistry of Xe is relatively well developed, while that of the lighter analogues is much less abundant, we focused on the Ar and Kr compounds in the present communication.

Computational Details

For the model systems, $\text{F}_3\text{Al} \leftarrow \text{Ng} \leftarrow \text{NH}_3$ scans of the potential energy surface (PES) have been performed using the Gaussian03 program package^{16a} using density functional theory (DFT) with the B3LYP¹⁷ hybrid functional in conjunction with the all electron def2-TZVPP¹⁸ basis set. For the selected points on the PES, single point computations have been performed at M05-2X¹⁹/def2-TZVPP (using Gaussian03 program package Rev. E.01^{16b}) and CCSD(T)²⁰/aug-cc-pVTZ (using Gaussian03 program package^{16b}).

- (7) (a) Khriachtchev, L.; Pettersson, M.; Runeberg, N.; Lundell, J.; Räsänen, M. *Nature (London)* **2000**, *406*, 874. (b) Khriachtchev, L.; Pettersson, M.; Lignell, A.; Räsänen, M. *J. Am. Chem. Soc.* **2001**, *123*, 8610.
 (8) Pettersson, M.; Khriachtchev, L.; Lignell, A.; Räsänen, M.; Bihary, Z.; Gerber, R. B. *J. Chem. Phys.* **2002**, *116*, 2508.
 (9) Wong, M. W. *J. Am. Chem. Soc.* **2000**, *122*, 6289.
 (10) Chen, Y.-L.; Hu, W.-P. *J. Phys. Chem. A* **2004**, *108*, 4449.
 (11) Belpassi, L.; Infante, I.; Tarantelli, F.; Visscher, L. *J. Am. Chem. Soc.* **2008**, *130*, 1048.
 (12) Breckenridge, W. H.; Ayles, V. L.; Wright, T. G. *J. Phys. Chem. A* **2008**, *112*, 4209.
 (13) Bucher, G. *Angew. Chem., Int. Ed.* **2003**, *42*, 4039.
 (14) Timoshkin, A. Y.; Frenking, G. *Organometallics* **2008**, *27*, 371.

- (15) Mück, L. A.; Timoshkin, A. Y.; Frenking, G. Manuscript in preparation.
 (16) (a) Frisch, M. J.; et al. *Gaussian03*, revision D.01; Gaussian, Inc.: Wallingford, CT, 2004. (b) Frisch, M. J.; et al. *Gaussian03*, revision E.01; Gaussian, Inc.: Wallingford, CT, 2004.
 (17) (a) Becke, A. D. *J. Chem. Phys.* **1993**, *98*, 5648. (b) Lee, C.; Yang, W.; Parr, R. G. *Phys. Rev. B* **1988**, *37*, 785.
 (18) Weigend, F.; Ahlrichs, R. *Phys. Chem. Chem. Phys.* **2005**, *7*, 3297.
 (19) (a) Zhao, Y.; Schultz, N. E.; Truhlar, D. G. *J. Chem. Theory Comput.* **2006**, *2*, 364. (b) Zhao, Y.; Truhlar, D. G. *Acc. Chem. Res.* **2008**, *41*, 157.

Due to the large computational costs required to compute complexes with cryptand ligands (which include up to 77 heavy atoms), initial geometry optimizations of cryptand ligands **1** and **1'** and their complexes have been carried out in framework of the C_{3v} point group at the RHF/6-31G* level of theory using Gaussian03.^{16a} Analytical evaluation of the second derivatives confirmed that obtained structures are true minima on the PES. For Ar@**1** and Kr@**1** additional geometry optimizations have been carried out using the Gaussian03 optimizer together with TurboMole5.8²¹ energies and gradients at the BP86²²/def2-TZVPP¹⁸ level of theory. The resolution-of-identity method²¹ has been applied using auxiliary basis sets from the TurboMole library. An ultra fine (multiple) grid m5 was used. For Ar@**1** and Kr@**1**, single point B3LYP/def2-TZVPP (using the multiple grid m4) and M05-2X/6-311G** energy computations have been carried out at RI-BP86/def2-TZVPP geometries. Basis set superposition error (BSSE) was estimated by the counterpoise method^{24a,b} realized in Gaussian03 for RHF/6-31G* and in TurboMole5.10 for B3LYP/def2-TZVPP level of theory. At RHF/6-31G* level of theory the BSSE value is only 6.5 kJ mol⁻¹ for the complex of Ar@**1'**. At the B3LYP/def2-TZVPP level of theory BSSE values are even smaller, 3.5 and 3.0 kJ mol⁻¹ for Ar@**1** and Kr@**1**, respectively. For the model compound NH₃-Ar-AlF₃, BSSE at B3LYP/def2-TZVPP is less than 3 kJ mol⁻¹. Given the fact that the counterpoise method generally overestimates BSSE,^{24c} in the following discussion we will use reaction energies, uncorrected for BSSE. Standard enthalpies were evaluated at the RHF-6-31G* level of theory taking into account zero point vibrational energy and thermal corrections using the rigid rotor-harmonic oscillator approximation. The difference between reaction energies at 0 K and reaction enthalpies at 298 K is less than 4 kJ mol⁻¹ (Table 2S, Supporting Information), and it should not change dramatically with the level of theory.

AIM analyses of the B3LYP/def2-TZVPP electron densities were performed using the AIMPAC program package.²⁵ NBO analyses²⁶ were performed at B3LYP/def2-TZVPP using the NBO3.1 module as implemented in Gaussian03. EDA analyses at BP86/TZ2P+ were performed using the decomposition scheme as implemented in ADF2007.1,^{27a} which adapts Morokuma's energy decomposition scheme^{27b} to Kohn-Sham molecular orbitals and uses the extended transition state partitioning scheme of the orbital interactions as developed by Ziegler and Rauk.^{27c}

Results and Discussion

In order to clarify a principal possibility of realization of the donor-acceptor induced 3-center 4-electron bond, a simple model system A ← Ng ← D was chosen for the investigation. Initially, we chose group 13 element fluorides BF₃, AlF₃ and

group 15 element hydrides NH₃, PH₃ as acceptor and donor molecules, respectively. Preliminary computations at the B3LYP/6-31G** level of theory, which included four possible combinations between acceptor molecules (BF₃ and AlF₃) and donor molecules (NH₃, PH₃) showed that the F₃Al-Ar-NH₃ combination is the best one in terms of interaction energies. Therefore, our further efforts were concentrated on the F₃Al-Ng-NH₃ system. Attempts of the full and partial (with frozen geometry of both donor and acceptor fragments) optimization of the F₃Al-Ng-NH₃ structure always led to the dissociation into the van der Waals bonded components. The influence of the destabilizing effect of the reorganization energies of the donor and acceptor molecules was excluded by artificially restricting both donor and acceptor moieties to the ideal tetrahedral environment (bond angles 109.471°). Eclipsed conformation, which is by a miniscule 0.01–0.04 kJ mol⁻¹ lower in energy, was used throughout. Preference for the eclipsed conformation is consistent with previous findings for the AlF₃NH₃ complex.²⁸ Both rigid and relaxed PES scans along Al-Ng and Ng-N coordinates have been performed. PES scans show strong repulsive Ng-NH₃ and weak attractive F₃Al-Ng interactions. Exothermicity of interaction energies increases in order He < Ne < Ar < Kr < Xe. PES scans revealed a shallow energy minimum with respect to the distance between the AlF₃ and Ng moieties (Figure 1S, Supporting Information), but no minimum for the distance between Ng-NH₃ moieties. The optimal Al-Ng distance is only slightly dependent on the Ng-N distance. Interaction of the tetrahedral fragments AlF₃ and NH₃ with Ng is much more energetically favorable compared to free AlF₃ and NH₃ molecules, mostly due to large pyramidalization energy of AlF₃ (90 kJ mol⁻¹ at B3LYP/def2-TZVPP level of theory). The formation of the complex with Ng does not compensate such an unfavorable preparation energy. Note that BF₃ forms with noble gases only very weak van der Waals complexes with negligible (~0.01) charge transfer.²⁹ Thus, it is important to conclude that, to form an energetically favorable complex with Ng, an acceptor molecule should be pyramidalized.

Energetic characteristics of the F₃Al-Ng-NH₃ systems at selected Ng-N and Al-Ng distances are summarized in Table 1. Bonding energies for Ar and Kr compounds, computed at the MP2(full)/def2-TZVPP level of theory, are by 10 kJ mol⁻¹ more exothermic compared to B3LYP values, indicating even stronger bonding between the components. Note that according to Li et al.³¹ MP2 overestimates the bond energies for Ar and Kr compounds. However, CCSD(T)/aug-cc-pVTZ results also show more exothermic complex formation energies than B3LYP/def2-TZVPP results. The difference between CCSD(T) and B3LYP increases from 1–3 kJ mol⁻¹ for He, to 5 kJ mol⁻¹ for Ne, to 10 kJ mol⁻¹ for Ar, and to ~20 kJ mol⁻¹ for Kr. Values obtained at M05-2X level of theory are close to the CCSD(T)/aug-cc-pVTZ results. Thus, we conclude that B3LYP/def2-TZVPP results provide the lower limit of the complex stability.

We have also performed an energy decomposition analysis (EDA) for the selected structures. For the EDA we choose the optimal Al-Ng distances (corresponding to the minima on PES scans); for Ng-N distance the value between the sum of the covalent and van der Waals radii³⁰ of Ng and N was chosen.

- (20) (a) Cizek, J. *J. Chem. Phys.* **1966**, *45*, 4256. (b) Pople, J. A.; Krishnan, R.; Schlegel, H. B.; Binkley, J. S. *Int. J. Quantum Chem.* **1978**, *14*, 545. (c) Bartlett, R. J.; Purvis, G. D. *Int. J. Quantum Chem.* **1978**, *14*, 561. (d) Purvis, G. D.; Bartlett, R. J. *J. Chem. Phys.* **1982**, *76*, 1910. (e) Raghavachari, K.; Trucks, G. W.; Pople, J. A.; Head-Gordon, M. *Chem. Phys. Lett.* **1989**, *157*, 479. (f) Bartlett, R. J.; Watts, J. D.; Kucharski, S. A.; Noga, J. *Chem. Phys. Lett.* **1990**, *165*, 513.
- (21) Ahlrichs, R.; Baer, M.; Haeser, M.; Horn, H.; Koelmel, C. *Chem. Phys. Lett.* **1989**, *162*, 165.
- (22) (a) Becke, A. D. *Phys. Rev. A* **1988**, *38*, 3098. (b) Perdew, J. P. *Phys. Rev. B* **1986**, *33*, 8822.
- (23) Eichkorn, K.; Treutler, O.; Ohm, H.; Haeser, M.; Ahlrichs, R. *Chem. Phys. Lett.* **1995**, *242*, 652.
- (24) (a) Boys, S. F.; Bernardi, F. *Mol. Phys.* **1970**, *19*, 553. (b) Simon, S.; Duran, M.; Dannenberg, J. J. *J. Chem. Phys.* **1996**, *105*, 11024. (c) Clark, T. *A Handbook of Computational Chemistry*; Wiley: New York, 1985.
- (25) Bader, R. F. W. *Atoms In Molecules Analysis Program for the PC*; <http://www.chemistry.mcmaster.ca/aimpac/imagemap/imagemap.htm>.
- (26) Reed, A. E.; Curtiss, L. A.; Weinhold, F. *Chem. Rev.* **1988**, *88*, 899.
- (27) (a) *ADF2007.01, SCM*; Theoretical Chemistry, Vrije Universiteit: Amsterdam, The Netherlands; <http://www.scm.com>. (b) Morokuma, K. *J. Chem. Phys.* **1971**, *55*, 1236. (c) Ziegler, T.; Rauk, A. *Theor. Chim. Acta* **1977**, *46*, 1.

- (28) Timoshkin, A. Y.; Suvorov, A. V.; Bettinger, H. F.; Schaefer, H. F. *J. Am. Chem. Soc.* **1999**, *121*, 5687.
- (29) Ford, T. A. *Spectrochim. Acta, Part A* **2005**, *61*, 1403.
- (30) Covalent and van der Waals radii are from: Huheey, J. E.; Keiter, E. A.; Keiter, R. L. *Anorganische Chemie*; Walter de Gruyter: Berlin, 1995.

Table 1. Comparative Characteristics of F₃Al–Ng–NH₃ Systems at Selected Ng–N and Al–Ng Distances^a

parameter	He		Ne		Ar		Kr		Xe	
$r_{\text{covAl}} + r_{\text{covNg}}$	1.62		1.99		2.27		2.40		2.60	
$r_{\text{covN}} + r_{\text{covNg}}$	1.07		1.44		1.72		1.85		2.05	
$r_{\text{vdwN}} + r_{\text{vdwNg}}$	3.35		3.15		3.45		3.55		3.75	
$r(\text{Ng–N}), \text{Å}$	1.8	3.2	2.2	3.4	2.4	3.6	2.6	3.8	2.7	3.9
$r(\text{Al–Ng}), \text{Å}$	1.765	1.95	2.065	2.135	2.38	2.43	2.54	2.585	2.735	2.79
q_{Ng}	0.144	0.092	0.138	0.102	0.219	0.191	0.214	0.193	0.221	0.212
$-q_{\text{AlF}_3}$	0.163	0.096	0.146	0.107	0.248	0.198	0.257	0.202	0.287	0.228
ΔE^{bond^b}	31.4	-22.3	5.5	-24.9	1.2	-44.8	-20.2	-48.9	-57.7	-77.5
	26.7 ^c	-28.2 ^c	-3.8 ^c	-33.3 ^c	-18.7 ^c	-61.7 ^c	-42.1 ^c	-67.9 ^c	-43.8 ^c	-73.9 ^c
	33.9 ^d	-23.4 ^d	2.9 ^d	-28.2 ^d	-7.6 ^d	-52.5 ^d	-39.7 ^d	-63.5 ^d		
	30.3 ^e	-25.8 ^e	0.1 ^e	-29.9 ^e	-8.6 ^e	-54.4 ^e	-40.6 ^e	-65.3 ^e		

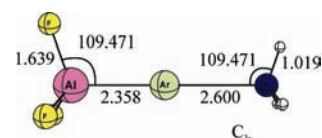
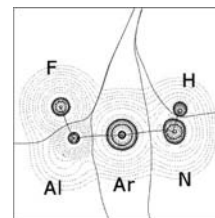
^a Ng–N distance is chosen close to the sum of covalent (left column) and van der Waals (right column) radii. Covalent and van der Waals radii of elements are taken from ref 30. B3LYP/def2-TZVPP level of theory. ^b Bonding energy ΔE^{bond} (kJ mol⁻¹) with respect to tetrahedral AlF₃ and NH₃. Positive sign corresponds to repulsive interactions (endothermic), and negative sign to attractive interactions (exothermic). ^c M05-2X/def2-TZVPP level of theory. ^d MP2/aug-cc-PVTZ level of theory. ^e CCSD(T)/aug-cc-PVTZ level of theory.

Table 2. Results of the EDA (BP86/TZVP+) and NBO (B3LYP/def2-TZVPP) Analyses for the Model Systems F₃Al–Ng–NH₃^a

parameter	He	Ne	Ar	Kr	Xe
$r(\text{Ng–N}), \text{Å}$	1.8	2.2	2.4	2.4	2.5
$r(\text{Al–Ng}), \text{Å}$	1.765	2.065	2.380	2.535	2.735
WBI ^b (Ng–N)	0.012	0.004	0.023	0.035	0.045
WBI ^b (Al–Ng)	0.172	0.127	0.262	0.317	0.376
$E_{\text{Pauli}}(\text{Ng–N})$	169.5	104.4	172.8	257.5	310.2
$E_{\text{Elstat}}(\text{Ng–N})$	-87.4	-74.6	-108.1	-156.3	-187.9
	(66.4%)	(88.4%)	(76.7%)	(74.7%)	(73.0%)
$E_{\text{orbital}}(\text{Ng–N})$	-44.2	-9.8	-32.9	-52.8	-69.4
	(33.6%)	(11.6%)	(23.3%)	(25.3%)	(27.0%)
$E_{\text{bond}}(\text{Ng–N})$	37.9	20.1	31.8	48.4	52.9
$E_{\text{Pauli}}(\text{Al–Ng})$	78.6	60.7	93.7	103.0	110.1
$E_{\text{Elstat}}(\text{Al–Ng})$	-74.9	-47.6	-68.4	-85.4	-92.9
	(53.4%)	(48.4%)	(40.9%)	(43.0%)	(42.2%)
$E_{\text{orbital}}(\text{Al–Ng})$	-65.5	-50.8	-98.8	-113.4	-127.0
	(46.7%)	(51.6%)	(59.1%)	(57.0%)	(57.8%)
$E_{\text{bond}}(\text{Al–Ng})$	-61.9	-37.8	-73.5	-95.9	-109.8
$q(\text{Ng})^c$	0.097	0.071	0.148	0.185	0.225
	0.144	0.138	0.219	0.207	0.208
$q(\text{AlF}_3)^c$	-0.122	-0.078	-0.170	-0.218	-0.263
	-0.163	-0.146	-0.248	-0.274	-0.308
$q(\text{NH}_3)^c$	0.025	0.001	0.022	0.034	0.038
	0.020	0.006	0.029	0.068	0.100
ΔE^{bond^d} BP86/ TZVP+	43.5	15.8	8.6	16.3	12.3
B3LYP/def2- TZVPP	31.3	5.5	1.2	24.7	17.0
M05-2X/def2- TZVPP	26.7	-3.8	-18.7	-0.7	-1.3
CCSD(T)/aug- cc-PVTZ	30.3	0.1	-8.6		

^a Geometries of the AlF₃ and NH₃ fragments are fixed ideal tetrahedral (as shown in Figure 1). Energies in kJ mol⁻¹. ^b Wiberg bond index. ^c NBO charges in the first row. Mulliken charges are in the second row. ^d Energy of the process AlF₃ + Ng + NH₃ = F₃Al–Ng–NH₃ (both AlF₃ and NH₃ in restricted tetrahedral geometry).

The results of EDA are presented in Table 2. The Pauli repulsion between Ng and NH₃ is dominant, resulting in endothermic Ng–N interaction. Ng–N bonding is mostly (66–88%) electrostatic, and orbital Ng–N interactions are small. This resembles the Ng–F interaction in H–Ng–F⁹ and Au–Ng–F.¹¹ In contrast, the bonding between AlF₃ and Ng is exothermic, and Al–Ng interaction is attractive and governed by orbital interactions, which increase in the order Ne < He < Ar < Kr < Xe. These findings clearly correlate with a well-pronounced minimum for the Al–Ng distance and absence of any minimum for Ng–N distance in our PES scans.

**Figure 1.** Geometry of the model of the cage F₃Al–Ar–NH₃, used for the Bader analysis.**Figure 2.** Laplacian of the electron density of F₃Al–Ar–NH₃ (geometry presented in Figure 1). Contour line diagrams $\nabla^2\rho(r)$ of F₃Al–Ar–NH₃ projected to F–Al–Ar–N–H plane. Solid line indicates areas of charge concentration ($\nabla^2\rho(r) < 0$), while dashed lines show areas of charge depletion ($\nabla^2\rho(r) > 0$). The thick solid lines connecting atomic nuclei are the bond paths, and those thick solid lines separating the atomic basins indicate the zero-flux surface crossing the F–Al–Ar–N–H plane.

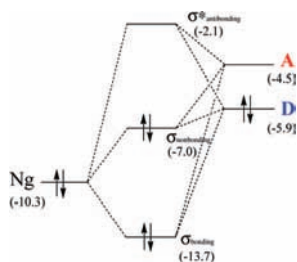
We have also analyzed the charge redistribution upon complex formation. Both Mulliken and NBO population analysis (Table 2) suggest that the noble gas always acts as a donor of the electron density and never acts as an acceptor. In contrast to the HNgF case, where significant charge transfer was evidenced,⁹ the charge transferred from the NH₃ moiety in F₃Al–Ng–NH₃ is very small. Wiberg bond indexes suggest the presence of the Al–Ng bond, while for the Ng–N bond Wiberg indexes are close to zero, in accord with the overall repulsive interactions found by EDA.

To get more insight into the nature of the interactions, an AIM bonding analysis for the model compound F₃Al–Ar–NH₃, in which both AlF₃ and NH₃ moieties are frozen and restricted to the ideal tetrahedral environment (Figure 1), has been performed. The Laplacian of the B3LYP/def2-TZVPP-electron density in the F–Al–Ar–N–H plane is presented in Figure 2. The Bader analysis clearly shows both Al–Ar and Ar–N bond paths, which is an indicator of a bonding between Ng and donor and acceptor molecules.

Analysis of the molecular orbitals of the model F₃Al–Ar–NH₃ compound (with restricted tetrahedral AlF₃ and NH₃), in which Al–Ar and Ar–N distances were fixed to the optimized values for Ar@1 (2.452 and 3.08 Å, respectively), reveals that primarily interaction between Al, Ng, and N atoms

(31) Li, T.-H.; Liu, Y.-L.; Lin, R.-J.; Yeh, T.-Y.; Hu, W.-P. *Chem. Phys. Lett.* **2007**, *434*, 38.

Scheme 3. Schematic Representation of the MO Diagram for the σ Orbitals of $A \leftarrow Ng \leftarrow D^a$



^aIn parentheses, values of respective orbital energies in eV for $F_3Al-Ar-NH_3$ system. (Al–Ar and Ar–N distances correspond to optimized values for Ar@**1**. RI-BP86/def2-TZVPP level of theory.)

indeed involves the formation of bonding, nonbonding, and antibonding σ orbitals as can be expected from the 3-center 4-electron bond (Scheme 3). Molecular orbitals with a contribution of the p-AO of Ar that points along the C_3 -axis of this model system are presented in Figure 3. Due to orbital contributions describing F–Al-bonding, an assignment of bonding, nonbonding, and antibonding orbitals with respect to the Al–Ar–N-interaction is not as straightforward as it is suggested in Scheme 3. In principle, the LUMO ($16a_1$) represents the main antibonding MO, the $14a_1$ MO represents the nonbonding combination, and the $12a_1$ the bonding combination (Figure 3). We conclude that the realization of the 3-center 4-electron bonding situation, depicted in Scheme 1b, is possible in principle. However, if the formation of a stable noble gas complex is desired, direct interactions between the donor and acceptor molecules should be suppressed. We propose that this may be achieved by using novel push–pull cryptand ligands based on tris(perfluoroaryl)aluminum and azaadamantane (Scheme 2).

The optimized geometries of cryptand **1** and its complexes with Ar and Kr are given in Figure 4, and their selected properties are listed in Table 3. Full optimization of Ar@**1** and Kr@**1** at RI-BP86/def2-TZVPP level of theory has been carried out without symmetry constraint, but the resulting structures are essentially C_{3v} symmetric. In the optimized structures, the Al–Ng and Ng–N distances are closer to the sum of the covalent radii of Ng and N, than to the sum of the van der Waals radii (Table 1). A notable feature of the acceptor pocket in **1** is the N–Al–C angle of 115.3° , which is much greater than the “ideal” tetrahedral angle 109.471° . This underlines the very large acceptor potential of **1**. Upon complex formation with Ng, the N–Al–C angle expectedly increases, but only by about 2° . This small increase is due to the rigid structure of **1**. Note that upon complex formation there is a small elongation of the Al \cdots N distance compared to the free cage; however, overall reorganization energy of the cage upon complex formation is less than 15 kJ mol^{-1} (Table 3). We must stress the importance of the rigidity of the cage in maintaining of the pyramidal for the acceptor center in the cryptand compound. Thus, an experimental attempt³² of practical realization of a 3-center 2-electron bond of the B–N–B type in the cage compound tris(2,6-dihydroxyphenyl)amine diborate resulted in intramolecular 2-center 2-electron dative B–N bond formation and inversion of the other boron atom with subsequent complexation with solvent THF molecule. In that case, theoretical computations predicted a desired 3-center 2-electron bonded structure to be a transition

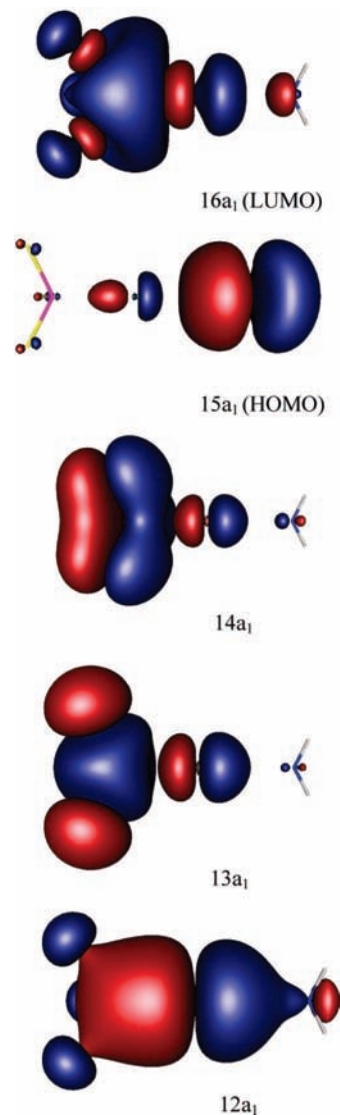


Figure 3. Kohn–Sham molecular orbitals of the model system $F_3Al-Ar-NH_3$ containing contributions of the argon-p-AO that points along the C_3 -axis of the system. Al–Ar and Ar–N distances correspond to optimized values for Ar@**1**. $15a_1$ is the HOMO of the system, and $16a_1$ is the LUMO. RI-BP86/def2-TZVPP level of theory.

state (TS).³² In our case, however, both free cryptand **1** and its complexes with Ng are true minima on PES.

Therefore, we consider the compounds presented in Figure 4b,c to be a true (genuine) stable chemical complex compound of the light noble gases Ar and Kr. Formation of both Ar@**1** and Kr@**1** is *exothermic* by about 20 kJ mol^{-1} both at the BP86 and B3LYP level of theory. At the M05-2X/6-311G** level of theory, formation of Ar@**1** and Kr@**1** is *exothermic* by 44.7 and 57.3 kJ mol^{-1} , respectively. Note that the standard enthalpy of formation of the most stable krypton compound KrF_2 from Kr and fluorine is endothermic.³ Matrix-isolated H–Ng–F compounds are also highly unstable thermodynamically with respect to Ng and HF formation.¹⁰

When discussing the thermodynamic stability of the noble gas compounds, one should keep in mind that their dissociation is entropically favorable. For the gaseous process $Ng@1 = Ng + 1$, predicted entropy change ΔS_{298}° lies in the range 115 – $125 \text{ J mol}^{-1} \text{ K}^{-1}$ at the RHF/6-31G* level of theory (Table 2S, Supporting Information). These values are smaller than the

(32) Livant, P. D.; Northcott, D. J.; Shen, Y.; Webb, T. R. *J. Org. Chem.* **2004**, *69*, 6564.

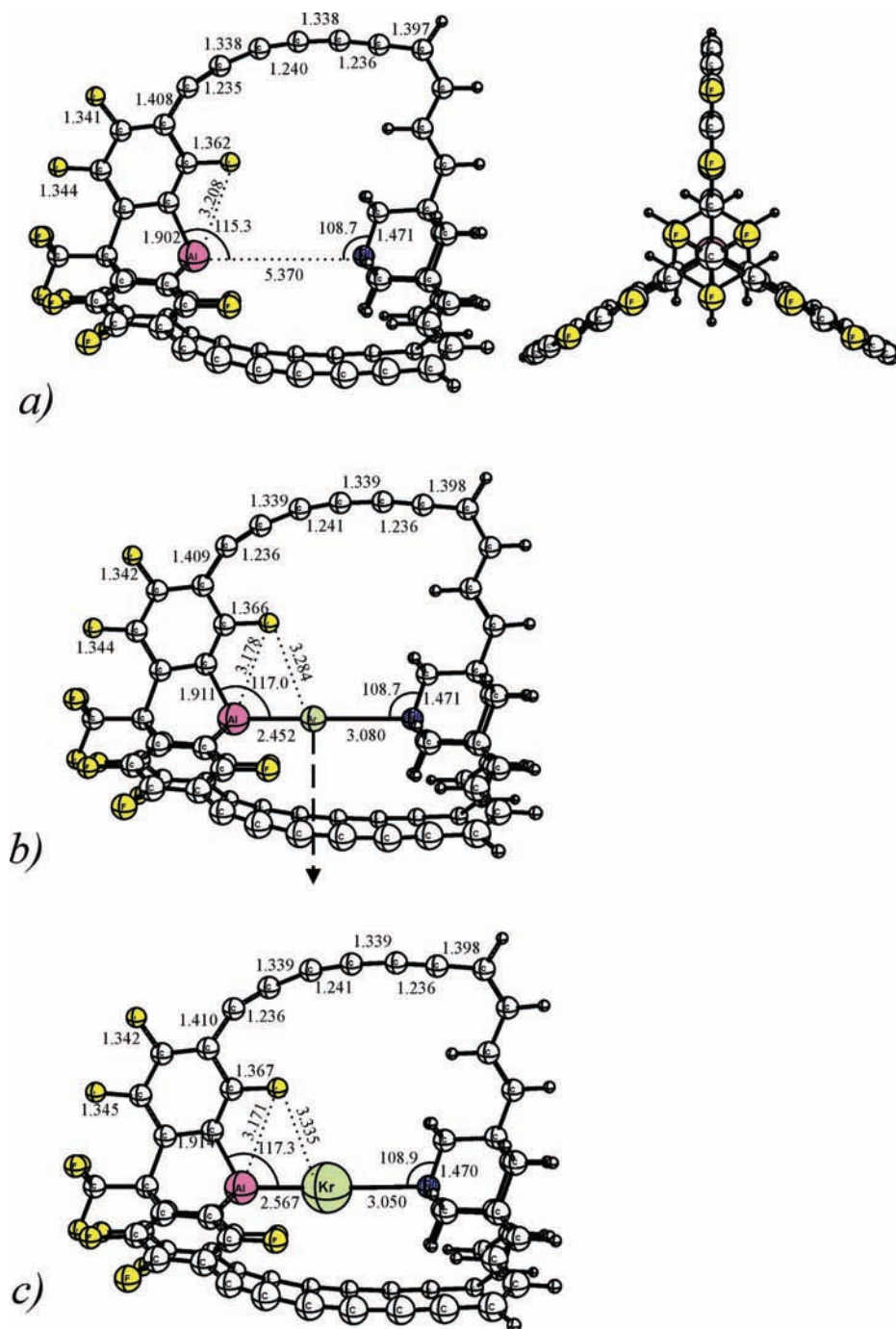


Figure 4. Optimized geometries (a) cryptand **1**, (b) Ar@**1**, and (c) Kr@**1**. All distances in angstroms, angles in degrees. RI-BP86/def2-TZVPP level of theory.

standard entropies of the gaseous Ar and Kr (154.8 and 164.1 $\text{J mol}^{-1} \text{K}^{-1}$, respectively).³³ Therefore, a value of the standard entropy of the respective noble gas can be used as an upper limit for the dissociation entropy.

Values of the Gibbs energy for the process $\text{Ng@1} = \text{Ng} + \mathbf{1}$ are positive at low temperatures (since dissociation reaction is endothermic), and therefore cryptand complexes Ng@1 are thermodynamically stable with respect to spontaneous Ng elimination at these conditions. In contrast, Gibbs energy values for the reactions of dissociation of other Ar and Kr compounds,

for example $\text{HArF} = \text{Ar} + \text{HF}$ or $\text{KrF}_2 = \text{Kr} + \text{F}_2$, are negative (since the process is both exothermic and entropically favorable), and such decomposition reactions are thermodynamically allowed at any temperature. Thus, HArF and KrF_2 are thermodynamically unstable with respect to the noble gas evolution at any temperature, while Ng@1 are *thermodynamically stable* at low temperatures.

It is known that dissociation of both thermodynamically unstable F-Ng-F and H-Ng-F compounds is kinetically protected by relatively high barriers.^{10,31} To address the kinetic stability of our cryptand complexes, we have performed a rigid PES scan of the noble gas extrusion from Ar@**1**. During the

(33) NIST Chemistry Webbook; *NIST Standard Reference Database Number 69*; June 2005 release; <http://webbook.nist.gov/chemistry/>.

Table 3. Characteristics of the Complexes of Cryptands **1** and **1'** with Ar and Kr^a

compd	point group	ΔE^{bond}	$r(\text{Al}-\text{Ng})$	$r(\text{Ng}-\text{N})$	$\Delta r(\text{Al}-\text{N})^c$	$q(\text{Ng})$	ΔE^{reorg}	level of theory
Ar@ 1'	C_{3v}	4.4	2.39	2.93	+0.67	0.129	13.4	RHF/6-31G*
Ar@ 1	C_{3v}	-5.5	2.43	3.04	+0.35	0.113	5.4	RHF/6-31G*
Ar@ 1	C_1^b	-17.5 (-19.9) ^d (-44.7) ^e	2.45	3.07	+0.15		2.9	RI-BP86/def2-TZVPP B3LYP/def2-TZVPP M05-2X/6-311G**
Kr@ 1'	C_{3v}	-30.0	2.48	2.93	+0.76	0.182	11.4	RHF/6-31G*
Kr@ 1	C_{3v}	-41.4	2.51	3.01	+0.40	0.168	8.3	RHF/6-31G*
Kr@ 1	C_1^b	-21.3 (-20.6) ^d (-57.3) ^e	2.57	3.06	+0.26			RI-BP86/def2-TZVPP B3LYP/def2-TZVPP M05-2X/6-311G**

^a Bonding energy ΔE^{bond} and cryptand reorganization energy ΔE^{reorg} are in kJ mol^{-1} , and distances are in angstroms. ^b Optimization was carried out without a symmetry constraint, but resulting structure is essentially C_{3v} symmetric. ^c Difference between the Al–N distance in the complex and in free cryptand. ^d Values are at B3LYP/def2-TZVPP/RI-BP86/def2-TZVPP level of theory. ^e Values are at M05-2X/6-311G**/RI-BP86/def2-TZVPP level of theory.

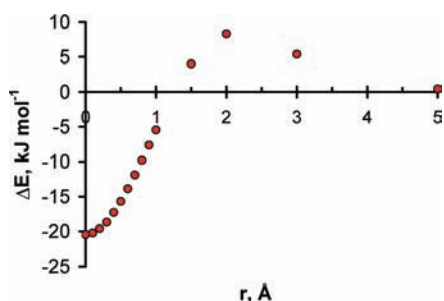


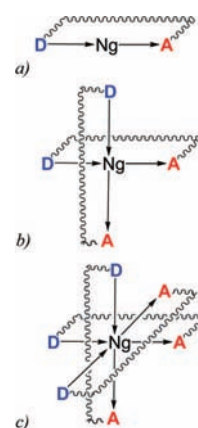
Figure 5. Rigid PES scan for the Ar removal from the Ar@**1** in the direction shown by the dashed arrow in Figure 4b. Relative energies with respect to the isolated Ar and **1** (in restricted geometry of the Ar@**1** complex). RI-BP86/def2-TZVPP level of theory.

scan, the geometry of **1** was fixed. Argon was moved out of the cage perpendicular to the Al–Ar–N axis (direction for the Ar extrusion is shown in Figure 4b by dashed arrow). The results (Figure 5) indicate that the Ar extrusion is protected by a barrier of 29 kJ mol^{-1} (RI-BP86/def2-TZVPP level of theory). A similar value of 20 kJ mol^{-1} was obtained at the RHF/6-31G* level of theory for the Ar extrusion from Ar@**1'**. We conclude that noble gas complexes with cryptands **1** and **1'** are kinetically protected by small ($20\text{--}30 \text{ kJ mol}^{-1}$) barriers.

Due to a large entropy contribution, the practical existence of Ar@**1** and Kr@**1** is possible only at low temperatures. The predicted values for the temperature, at which dissociation pressure of the complex equals the partial pressure of the respective noble gas in the atmosphere ($\sim 10^{-2}$ and $\sim 10^{-6}$ atm for Ar and Kr, respectively), are 160 and 110 K for Ar@**1** and Kr@**1**, respectively (using B3LYP results for the reaction enthalpy). Of course, an increase of the partial pressure of the noble gas will shift the equilibrium toward formation of Ng@**1**. Thus, complex formation is expected to proceed at low temperature–high pressure conditions.

We must also stress that complexation energy has a dominant effect on the stability of the compounds. Upon an increase of the exothermicity of complex formation by merely 10 kJ mol^{-1} , the temperature stability window will be increased by 40–60 K. In fact, taking reaction enthalpies predicted at the M05-2X/6-311G** level of theory, one can conclude that both Ar@**1** and Kr@**1** are thermodynamically stable with respect to Ng extrusion at room temperature. We suggest that the application of the push–pull ligands which feature multiple (two or three) donor–acceptor induced 3-center 4-electron bonds (Scheme 4) may result in even larger stabilization of the complex. Thus, it is expected that further progress in the design of the push–pull cryptands with rigid pyramidalized donor–acceptor pockets may

Scheme 4. Schematic representation of the formation of the donor–acceptor complexes, featuring (a) one, (b) two, and (c) three 3-center 4-electron DA bonds. Wavy lines represent rigid connection between donor and acceptor center



lead to DA complexes of Ar and Kr which will be stable at room temperatures. Further theoretical investigations on the topic are currently underway.

Conclusions

The concept of the formation of a donor–acceptor 3-center 4-electron bond has been introduced into the chemistry of noble gases. Bonding analysis for the model $\text{F}_3\text{Al}-\text{Ng}-\text{NH}_3$ systems reveals that the Al–Ng interaction has large orbital components while the Ng–N interaction shows a relatively large electrostatic contribution. Practical realization of this concept requires the design of a ligand which features spacially divided and prearranged (pyramidal) donor and acceptor pockets. It is shown that model ligand **1** is predicted to exothermically form complexes both with argon and krypton. These complexes are the first examples of the *thermodynamically stable* chemical compounds in Ar and Kr chemistry. They are also the first examples of compounds featuring Al–Ar and Al–Kr bonds.

Beyond formation of the noble gas complexes, the concept of the donor–acceptor 3-center 4-electron bond could open a new dimension to coordination chemistry in general. On the basis of our successful effort for the design of the push–pull cryptand ligand, which is predicted to exothermically interact with noble gases, we are optimistic that it would be possible to design corresponding donor–acceptor cryptand ligands for any given electron-rich element in the periodic table. Our theoretical predictions await experimental realization.

Acknowledgment. A.Y.T. is grateful to the Alexander von Humboldt Foundation for sponsorship of his short-term visit to

Philipps-Universität Marburg. L.A.M. is grateful to DAAD for sponsorship of her visit to St. Petersburg State University. The excellent service of the MARC computer cluster of Philipps-Universität Marburg is gratefully acknowledged.

Supporting Information Available: Complete ref 16 citation; table with complexation energies of $F_3Al-Ar-NH_3$ at different levels of theory; figure with PES scans for the model compounds; table with thermodynamics characteristics for the gas

phase reactions of complex dissociation at RHF/6-31G* level of theory; total energies of the compounds at different levels of theory; and Cartesian coordinates of **1**, Ar@**1**, and Kr@**1** at RI-BP86/def2-TZVPP and RHF/6-31G* levels of theory. This material is available free of charge via the Internet at <http://pubs.acs.org>.

JA805990H